RevMexAA (Serie de Conferencias), **36**, 17–24 (2009)

SUPERNOVA EXPLOSIONS AND THE TRIGGERING OF GALACTIC FOUNTAINS AND OUTFLOWS

E. M. de Gouveia Dal Pino,[1] C. Melioli,[1,2] A. D'Ercole,[2] F. Brighenti,[3] and A. C. Raga[4]

RESUMEN

Damos una reseña de los efectos de explosiones de supernovas (SNe) sobre el medio ambiente de galaxias con formación estelar. Explosiones de SNe en cúmulos distribuidos al azar producen super burbujas calientes que impulsan fuentes galácticas o vientos supersónicos que salen del disco galáctico, dependiendo de la cantidad y concentración de la energía que inyecten. En una fuente galáctica, el gas eyectado es recapturado por el potencial gravitacional, y vuelve a caer sobre el disco. Con simulaciones 3D de dinámica de gases radiativos fuera de equilibrio de estas fuentes galácticas, encontramos que pueden llegar a alturas menores a 5 kpc en el halo, y de esta manera explicar las nubes de velocidad intermedia (IVCs) frecuentemente observadas sobre los discos de estas galaxias. Por otro lado, las nubes de alta velocidad (HVCs) observadas a mayores alturas (hasta de 1 kpc) requieren de otro mecanismo para explicar su producción. Argumentamos que podrían ser formadas por captura de gas del medio intergaláctico y/o por la acción de campos magnéticos llevados hacia el halo con el gas de las fuentes galácticas. Debido a pérdidas de momento angular (de 10–15%) al halo, encontramos que el material de las fuentes cae sobre radios menores, y no es esparcido sobre el disco, como era esperado, cayendo en vez cerca de la región donde está la fuente. Este resultado es consistente con la distribución de metales de recientes modelos químicos de la galaxia. También encontramos que después de aproximadamente 150 Myr la circulación del gas entre el halo y el disco en las fuentes llega a un estado estacionario, el cual es poco sensible a la distancia de las fuentes al centro galáctico. El material que vuelve a caer sobre el disco lleva a la formación de nuevas generaciones de estructuras complejas que alimentan la turbulencia supersónica del disco.

ABSTRACT

We review here the effects of supernovae (SNe) explosions on the environment of star-forming galaxies. Randomly distributed, clustered SNe explosions cause the formation of hot superbubbles that drive either galactic fountains or supersonic winds out of the galactic disk, depending on the amount and concentration of energy that is injected by them. In a galactic fountain, the ejected gas is re-captured by the gravitational potential and falls back onto the disk. From 3D non-equilibrium radiative cooling hydrodynamical simulations of these fountains, we find that they may reach altitudes smaller than 5 kpc in the halo and hence explain the formation of the so-called intermediate-velocity-clouds (IVCs) often observed above the disk of these galaxies. On the other hand, the high-velocity-clouds (HVCs) that are observed at higher altitudes (of up to 12 kpc) require another mechanism to explain their production. We argue that they could be formed either by the capture of gas from the intergalactic medium and/or by the action of magnetic fields that are carried out to the halo with the gas in the fountains. Due to angular momentum losses (of 10–15%) to the halo, we find that the fountain material falls back to smaller radii and is not largely spread over the galactic disk, as previously expected, but falls near the region where the fountain was produced This result is consistent with the metal distribution derived from recent chemical models of the galaxy. We also find that after about 150 Myr, the gas circulation between the halo and the disk in the fountains reaches a steady state regime, and this is relatively insensitive to the galacto-centric distance where the fountains are produced. The fall back material leads to the formation of new generations of complex structures that help to feed the supersonic turbulence in the disk.

Key Words: Galaxy: galactic fountains — Galaxy: winds — ISM: supernovae explosions — ISM: superbubbles

1. INTRODUCTION

Edge-on star forming disk galaxies often exhibit hot halos of ionized gas that may extend for sev-

[1]Instituto Astronomico e Geofisico, Universidade de Sao Paulo, IAG-USP, R. do Matao, 1226, Cd. Universitaria, Sao Paulo, SP, Brazil (dalpino@astro.iag.usp.br).

[2]INAF-Osservatorio Astronomico di Bologna, via Ranzani 1, 40126 Bologna, Italy.

[3]Dipartimento di Astronomia, Universita di Bologna, via Ranzani 1, 40126 Bologna, Italy.

[4]Instituto de Ciencias Nucleares, Universidad Nacional Autónoma de México, Apdo. Postal 70-543, C.P. 04510, D.F., México.

eral kpc above the regular HI galactic disk. They are fed by ascending gas from the disk in structures that resemble chimneys and fountains. Observations indicate that the chimneys are generated by supernovae (SNe) explosions which blow superbubbles that expand and carve holes in the disk, injecting high speed, metal enriched gas that forces its way out through relatively narrow channels with widths of 100–150 pc. They establish a connection between the thin disk and the halo, feeding it with the hot disk gas that expands under buoyancy forces up to a maximum height into the halo and then returns to the disk, pulled by the disk gravity. The whole cycle is like a fountain — hence the name galactic fountain. Evidence for large chimneys is clear in external galaxies in the form of holes and flows in the distribution of HI. In the Milky Way (MW), the evidence has mainly been in the form of fragments and vertical structures in the large scale maps of the interstellar medium. A multi-wavelength survey of the halos of several star forming galaxies (e.g., Dettmar 2005) have revealed a correlation of these halos with the rates of star formation and the energy input rates by SNe, suggesting that gaseous halos are associated to star formation processes in the disk.

Other observed features that seem to be correlated to gas circulation in chimneys and galactic fountains are the so-called intermediate and high-velocity-clouds (IVCs and HVCs, respectively). These are mainly neutral hydrogen (HI) clouds that can be as large as 100 pc, with masses of up to 10^4 $M_\odot$ that are observed in the halo of the MW and other star forming galaxies at altitudes typically between 300 pc and 2.5 kpc, which are falling on the disk with velocities between -20 km/s and -90 km/s. The HVCs can be observed at even higher altitudes (up to 12 kpc) and with velocities of up to -140 km/s. Figure 1 provides a mosaic of the matter distribution in the halo of the MW (see also de Gouveia Dal Pino et al. 2008) which shows that the galactic disk is surrounded by a very cloudy environment. It is generally believed that at least the IVCs have been formed from the condensation of the gas that arises in the chimneys triggered by SN explosions, and numerical simulations seem to confirm this hypothesis (e.g., de Avillez 2000; de Avillez & Breitschwerdt 2005; Melioli et al. 2008a; Melioli et al. 2008b; see below). However, the origin of the HVCs is still controversial. The difficulty at producing fountains (in hydrodynamical simulations) reaching altitudes higher than 5 kpc (Melioli et al. 2008b) and the very small metallicity contents observed in these HVCs suggest that they may have originated

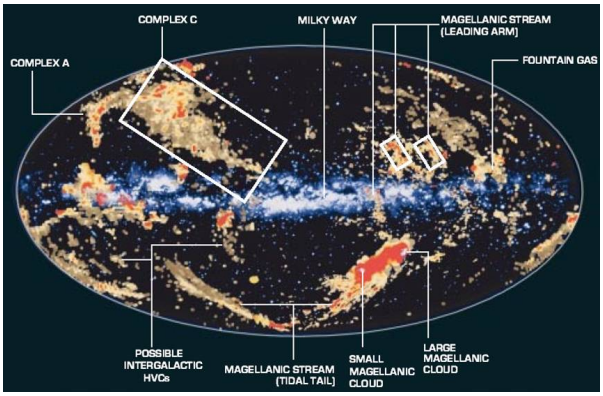

Fig. 1. Map of the galactic gas and its environment that combines radio observations of neutral hydrogen (HI) of the environment with a visible light image of the MW (the galactic disk is in the middle). The high and intermediate-velocity clouds of hydrogen, such as complexes A and C, are located above and below the disk. A galactic fountain is also identified in the map (extracted from `http://www.astro.uni-bonn.de/~webiaef/outreach/posters/milkyway/`).

from gas raining into the galaxy, accreted from the intergalactic medium (IGM) or from satellite galaxies (e.g., Fraternali & Binney 2006).

Other examples of violent gas outflows coming out of the disk of star forming galaxies are the supersonic winds, which are powerful enough to escape from the gravitational potential of the galactic disk to the IGM. A large-scale bipolar wind seems to be emerging from the center of the MW (Bland-Hawthorn & Cohen 2003) and spectacular winds extending for several kpc above the disk have been observed in galaxies with bursts of star formation. These starburst (SB) galaxies are actually merging or interacting galaxies that can have star formation rates up to 20 times larger than those of regular galaxies, and this could explain the large amount of energy injection by SNe and the resulting production of powerful winds. Galactic winds are indeed ubiquitous in SBs (Veilleux, Cecil, & Bland-Hawthorn 2005, and references therein). Recent, high resolution observations of the best studied prototype of this class, the Starburst galaxy M82, show evidence that its wind, as in galactic fountains, is being fed by SNe explosions nestled in several stellar associations around the nuclear region of the galaxy (Konstantopoulos et al. 2008). In this brief review, we will focus on the formation of galactic fountains and thus will not address any further these powerful galactic winds, but we refer to, e.g., Melioli & de Gouveia Dal Pino (2004) and Cooper et al. (2008, and refer-

ences therein) for a more complete discussion of the efficiency of the SNe in powering the SBs and their outflow production.

Extensive work on the formation of galactic chimneys and fountains has been carried out over the last decades (see e.g., de Avillez 2000; de Avilles & Breitschwerdt 2005; Melioli et al. 2008a, and references therein for reviews). Shapiro & Field 1976 first proposed the idea that galactic chimneys induced by SNe explosions would cause gas circulation between the disk and the halo. This scenario was afterwards explored analytically in detail by Bregman (1980) and Kahn (1981). More recently, the advent of powerful computers have made it possible to simulate fountains and winds rather accurately. The first 3D hydrodynamical simulations following the whole cycle of the gas between the disk and the halo in fountains in the MW were performed by de de Avillez 2000 and de de Avillez & Berry (2001). However, in order to obtain a high spatial resolution, they considered only a small region of the Galaxy with a dimension of 1 kpc^2 (in the disk) $\times$ 10 kpc (for the height in the halo). Korpi et al. (1999) have included the effects of the differential rotation and the magnetic field of the galactic disk, but considered a computational domain too small (500 pc^2 $\times$ 1 kpc) to allow for the development of an entire cycle of the chimney gas between the disk and the halo. Other works that were also concerned with the collective effects of supernovae on the structure of the interstellar medium (ISM) have considered even smaller volumes in their hydrodynamical simulations (see, e.g., Mac Low, McCray, & Norman 1989). More recently, further MHD simulations were carried out by de Avillez & Breitschwerdt (2005), without including differential rotation, where again, in order to reach very high resolution (of 0.6 pc) they considered only a small volume of the Galaxy (1 kpc$^2\times$ 10 kpc), as they were primarily concerned at examining the role of the disk-halo gas circulation in establishing the volume filling factors of the different phases of the ISM in the Galactic disk. In particular, these MHD studies have revealed that the gas transport into the halo is not prevented by the parallel magnetic field of the Galaxy (as suggested in former works; see e.g., Tomisaka 1998), but only delayed by few tens of Myr when compared to pure HD simulations.

In the following sections, we summarize the results of a recent study of the large scale development of galactic fountains driven by SNe explosions, which was carried out in order to understand their dynamical evolution, the observed kinematics of the extraplanar gas, the formation of IVCs and HVCs, and the influence of the fountains in the redistribution of the freshly delivered metals over the galactic disk. To this aim, we have performed fully 3D, non-equilibrium radiative cooling hydrodynamical simulations of the gas in the Milky Way, in which the whole Galaxy structure, the galactic differential rotation, the total (thermal + magnetic) pressure, and the supernovae explosions generated in single and multiple stellar associations of OB stars have been considered (see Melioli et al. 2008a,b for more details). We will also discuss qualitatively the dynamical influence that the magnetic fields are expected to have on these outflows.

2. NUMERICAL SIMULATIONS

The initial numerical setup is described in detail in Melioli et al. (2008a,b). The ISM is initially set in rotational equilibrium in the galactic gravitational potential, given by the addition of the dark-matter halo, the bulge, and the disk contributions. Assuming hydrostatic equilibrium in the z- (vertical) direction between gravity and the full pressure (given by the thermal gas + magnetic + cosmic ray pressure contributions), we have computed the rotation velocity as a function of the galacto-centric distance R. This allowed us to build the full galactic rotation curve, as observed in the MW for different z heights. The ISM in our model is made up of the three gas components, namely the molecular (H_2), the neutral (H I) and the (H II) hydrogen components, and their stratified density distribution follows the empiric curves obtained for the MW by Wolfire et al. (2003). In most models, a hot ($T_h = 7 \times 10^6$ K) isothermal gas halo was added, in equilibrium with the galactic potential well. In some models the halo was allowed to rotate with a velocity that was a fraction of the disk velocity.

In order to drive the formation of chimneys and fountains, we have considered two sets of models. In one set, we continuously exploded 100 SNe over 30 Myr in a single star cluster. In a second set, we randomly exploded up to 2000 SNe in multiple star clusters (spread over an area of either 1 kpc^2 or 8 kpc^2 on the disk). In both cases, the clusters were generally localized at a radial distance R =8.5 kpc, which corresponds to the distance between the Sun and the galactic center. We have assumed the SNe rate distribution over time that has been inferred from observations of the MW (Higdon & Lingenfelter 2005).

The simulations employ a modified version of the adaptive mesh refinement YGUAZU code that in-

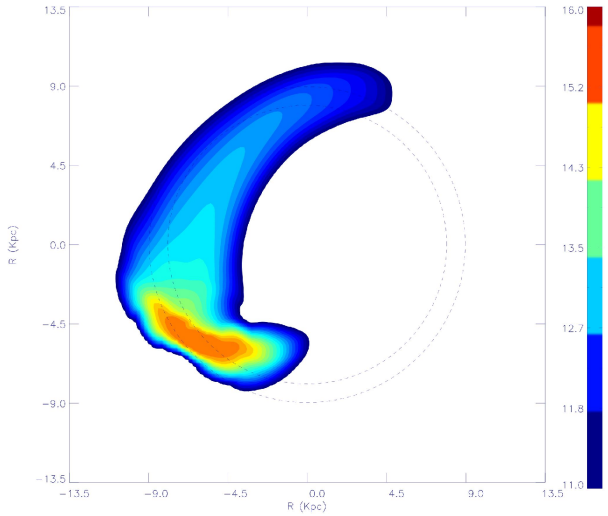

Fig. 2. Face-on view of the z-column density distribution of the SN ejecta after $t = 160$ Myr for a single fountain. The SNe explode at a radius $R = 8.5$ kpc, halfway between the radii $R = 8$ kpc and $R = 9$ kpc of the two circles drawn in the figure to guide the eye. Their distance represents approximately the maximum extension of the hole in the ISM carved by the fountain on the disk during its activity. At the depicted time, the hole has collapsed and disappeared. The column density scale is given in cm^{-2} and the x, y axes are labeled in kpc (from Melioli et al. 2008a).

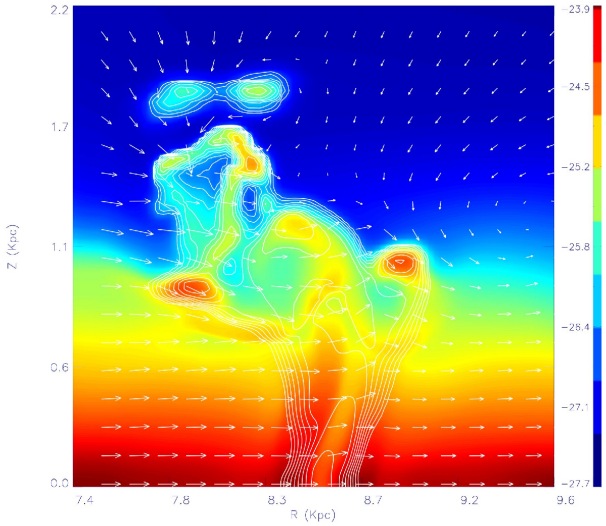

Fig. 3. Edge-on view of the single fountain of Figure 1 at $t = 50$ Myr, when the ascending gas reaches its maximum height ($z = 2$ kpc). Isodensity curves of the ejecta are superimposed on the disk gas density distribution, highlighting the fountain pattern and the cloud formation (see the text; from Melioli et al. 2008a.)

tegrates the 3D invisced gasdynamic equations with the flux vector splitting algorithm of van Leer (Raga, Navarro-González, & Villagrán-Muniz 2000; Raga et al. 2002; see also, e.g., González et al. 2004; Melioli, de Gouveia Dal Pino, & Raga 2005). The non-equilibrium radiative cooling of the gas is computed together with a set of continuity equations for atomic/ionic or chemical species. The 3D binary, hierarchical computational grid has a uniform base grid, and a number of higher resolution grids at chosen spatial positions. We have enforced the maximum grid resolution only in the volume encompassed by the fountain. In order to follow the circulation and the thermal history (i.e., the degree of radiative cooling) of the metals expelled by the SNe, we have added three different tracers passively advected by the code describing the disk gas, the halo gas, and the SNe ejecta (see Melioli et al. 2008a for details).

Figures 2 and 3 exhibit the face-on and edge-on views of the evolution of a galactic fountain arising from SNe explosions within a single OB association located at the galacto-centric distance $R = 8.5$ kpc. At this radius the transition between the disk and the hot halo occurs at $z = 800$ pc. The critical luminosity for the SNe to break through the disk is $L_b \simeq 1.5 \times 10^{37}$ erg/s (e.g., Koo & McKee 1992), which is well below the mechanical luminosity $L_W = 10^{38}$ erg/s provided by the 100 SNe powering the fountain. This model was run with a maximum spatial resolution of 12.5 pc.

During its activity, the fountain digs a hole in the disk and throws SNe ejecta and ISM vertically up to $z \sim 2$ kpc above the galactic plane. Once the explosions cease, the hole collapses in 2×10^7 yr and the ejecta trapped at its edges (nearly half of the total) mixes with the local ISM. Owing to the differential rotation of the Galactic disk, the ejecta is not confined to one spot, but is stretched, giving rise to the bean-like structure seen in Figure 2. The low density tail with a banana-shape is due to the ejecta pushed at high altitudes which then slowly falls back, remaining above the disk. The two concentric circles in Figure 2 with radii $R = 8$ kpc and $R = 9$ kpc, have been drawn to guide the eye. The SNe explode between these two circles, and their distance corresponds to the diameter of the hole produced by the fountain. Comparing the shape of the tail traced by the ejecta with the circles, we note that the gas of the fountain tends to move inward during its trajectory. Actually, as the gas moves upward and interacts with the halo, it transfers to it part of its angular momentum; the centrifugal force decreases in pace with the circular velocity and gravity prevails, pushing the gas toward the Galactic center (see Figure 3).

Further insight on the evolution of the galactic fountain is obtained from Figure 4, which illustrates several quantities starting from $t = 30$ Myr, the time at which the SNe stop exploding. The upper panel shows how quickly the ejecta looses its angular momentum because of the interaction with the gaseous halo. After 80 Myr, nearly 10% of the angular momentum of the fountain has been transferred to the hot halo; later on, no further transfer occurs because nearly 75% of the ejecta is located below the disk-halo transition and rotates together with the ISM. The middle panel of Figure 4 shows the ejecta mass fraction located above different heights. It is interesting to note that for $t > 80$ Myr, the long-term evolution of these quantities becomes very slow. This is due to the fact that most of the ejecta situated above the plane is rather diluted and tends to float together with the extra-planar ISM. Finally, in the lower panel of Figure 4, we quantify the tendency of the ejecta to move radially by plotting the fraction of the total mass of ejecta located at $R < 9$ kpc and $R > 8$ kpc (i.e. the radii of the two circles drawn in Figure 2); the amount of mass located within the region $8 \leq R \leq 9$ kpc is not taken into account. In the beginning, the ejecta starts to follow the expected tendency to move outward but, as the loss of angular momentum proceeds, the fraction of gas moving inwards increases, and after 60 Myr overrides the outward directed mass transport.

The gas lifted up by the fountain has a mass of 2.5×10^5 $M_\odot$, almost all (92%) condensed in dense filaments cooled to $T = 10^4$ K (see Figure 3). The clouds form via thermal instabilities at $z \sim 2$ kpc, the maximum height that the ascending gas reaches before starting to move back toward the disk at 50 Myr. All the clouds have negative z-velocities in the 50–100 km/s range. The chemical composition of these clouds is practically unaffected by the SN ejecta. The fountain is powered by 100 SNe, half of them exploding in the half space mapped by the grid; as each supernova delivers on average 3 $M_\odot$ of metals, a total of 150 $M_\odot$ of heavy elements is ejected by the fountain in Figures 2 and 3. yOnly 20% of the metals of the ejecta is locked in the clouds, 50% of this material remains trapped within the disk and 30% remains floating over the disk as hot, diffuse gas. As a result, the metallicity increment in the clouds due to the freshly delivered metals corresponds to 0.01 in solar units and is negligible compared to the solar abundance of the ISM. As we will show below, this result also holds in models with multiple SNe associations. In conclusion, almost all the gas lifted up by the fountain condenses into clouds without being chemically affected. After 150 Myr, 45% of the fresh metals stays on the disk (below $z = 800$ pc) within a radial distance of $R = 0.5$ kpc from the OB association. A fraction of 35% is found on the disk within the $9.5 < R < 7$ kpc range. The

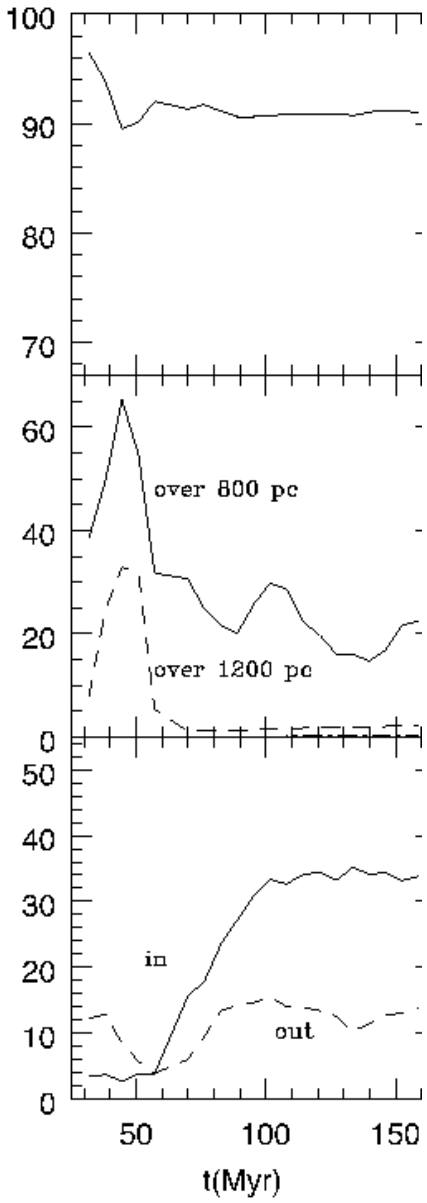

Fig. 4. The upper panel shows the evolution of the angular momentum of the SN ejecta for the single galactic fountain of Figures 2 and 3. The evolution of the amount of the ejecta above different heights is illustrated in the middle panel. The lower panel displays the temporal behavior of the amount of ejecta located at $R < 8$ kpc (dashed line) and $R > 9$ kpc (solid line); these two radii correspond to the circles visible in Figure 2 (from Melioli et al. 2008a).

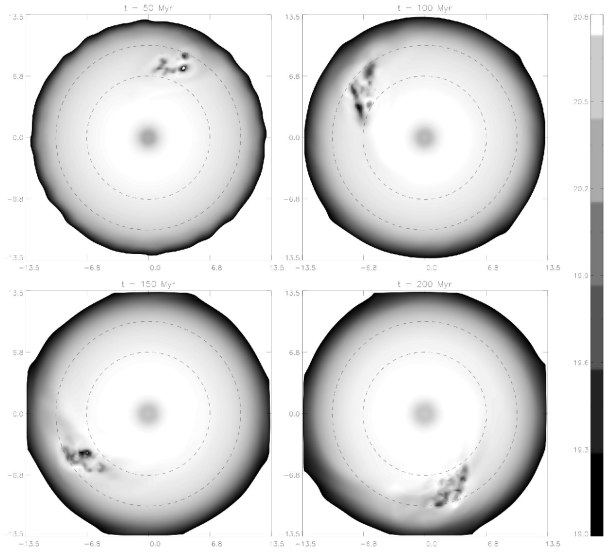

Fig. 5. Face-on view of the evolution of a multiple fountain triggered by the explosion of SNe from randomly distributed stellar clusters over an area of 8 kpc^2 of the galactic disk at a distance $R = 8.5$ kpc from the galactic center. The figure shows 4 snapshots of the evolution of the column density (in cm^{-2}) of the ascending gas (ISM+SNe ejecta) in a multiple fountain (from Melioli et al. 2008b).

remaining 20% of metals is still over the disk, half of which is at $R > 8.5$ kpc and half at $R < 8.5$ kpc.

Figure 5 shows the results for a multiple fountain model that was produced by randomly clustered explosions of SNe originating in stellar associations spread over a disk area of 8 kpc^2 for a period $P = 200$ Myr with a mean rate adequately scaled from the rate of 1.4×10^{-2} yr^{-1} for the whole Galaxy (Cappellaro et al. 1997). During the time P of the simulation, $N_{\rm tot} = 1.59 \times 10^4$ SNe exploded in the active area of the Galactic disk. The employed size-frequency distribution of the clustered SNe progenitors follows the distribution inferred from observations by Higdon & Lingenfelter (2005) for the MW.

We may notice the holes dug by the SNe into the disk in the beginning, at $t = 30$ Myr. As time goes by, as in the case of the single fountain (of Figures 2 and 3), the ascending material in the multiple fountains is stretched by the rotation, forming cometary tail-like structures. Again, as the ascending material returns to the disk it tends to fall towards the inner disk region due to angular momentum losses (of about 15%) to the halo. In this case, the maximum height attained by the fountain material, with the formation of dense cold clouds from the condensation of the hot gas, is two times larger than in the case of the single fountain, and the clouds rain back on the disk with velocities between -50 km/s and -100 km/s. Hence, these results indicate that the galactic fountains are able to produce only IVCs. We have also found that these results are relatively insensitive to the distance of the fountains to the galactic center (they were also simulated at a distance of 4.5 kpc from the galactic center). Our simulations of multiple fountains have also revealed that the amount of gas circulating between the halo and the disk reaches a dynamical equilibrium around 150 Myr, so that after this time the amount of gas falling back on the disk is approximately equal to the gas ascending in the fountain (Figure 6). As before, the spreading of the SNe ejecta falling back on the disk is not very large. Most of the gas lifted by the fountain falls back within a distance $\Delta R = \pm$ 0.5 kpc from the place where the fountain was originated. This is in agreement with recent chemical models of the metal distribution in the MW disk (Cescutti et al. 2007).

3. CONCLUSIONS AND DISCUSSION

Large scale 3D hydrodynamical, non-equilibrium radiative cooling simulations of random explosions of SNe in off-center stellar clusters in a rotating galactic disk-bulge system evidence the formation of giant superbubbles that break through the galactic disk into the halo, forming chimneys and fountains:

- The gas lifted by multiple fountains condenses into clouds that reach altitudes smaller than 5 kpc and then fall back into the disk with velocities between ~ -50 km/s and -100 km/s. These clouds can thus explain the formation of the IVCs, but not of the HVCs that are observed at heights as large as 12 kpc in the halo. After about 150 Myr, the gas circulation between the halo and the disk in the fountains is found to reach a steady state regime, which is relatively insensitive to the galacto-centric distance where the fountains are produced.
- After a maximum lift, the clouds rain back on the disk, but towards smaller radii due to angular momentum losses (10%–15%) to the halo. This amount of angular momentum may be large enough to provoke an eventual co-rotation of the halo with the disk. However, the observed halos of star forming galaxies often show a rotational velocity gradient with respect to the disk of $\Delta v_{\rm rot} \simeq -15$ km/s/kpc (for $1.3 < z < 5.2$ kpc; Dettmar 2005). This could be an indication that some other mechanism (possibly of external origin) might be operating to inhibit the halo rotation (see more details in Melioli et al. 2008b).

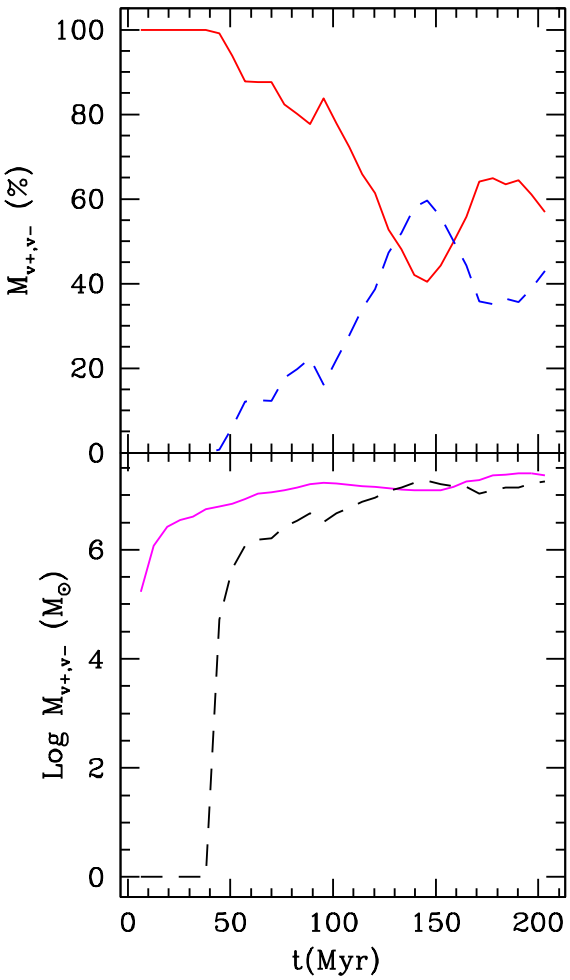

Fig. 6. Disk-halo gas circulation in the multiple fountain model of Figure 5. The amount of gas going up (continuous line) and down (dashed line) reaches a dynamical equilibrium around 150 Myr (from Melioli et al. 2008b).

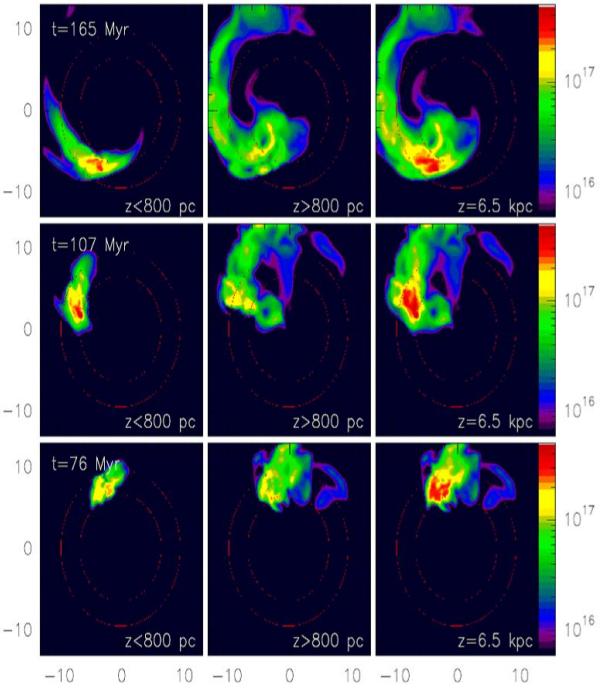

Fig. 7. Multiple fountain + IGM combined matter infall. Face-on view of the evolution of the multiple fountain triggered by the explosion of SNe from randomly distributed stellar clusters over an area of 8 kpc^2 of the galactic disk at a distance $R = 8.5$ kpc from the galactic center, as in Figure 5, but including infalling gas accreted from the IGM at a $dM/dt = 1 \rightarrow 2\ M_\odot$ yr^{-1} rate. The figure shows 3 snapshots of the evolution up to 165 Myr of the column density distribution (in cm^{-2}) of the (ascending + infalling) gas, at 3 different heights above the disk. In this case we can see the formation of high-velocity structures at heights larger than 5 kpc due to the infall (from Melioli et al. 2008b).

• The galaxy rotation inhibits both a straight vertical expansion of the fountains and the spreading of the metals transported by the fountains from the SNe. Contrary to ballistic models, most of the gas that is lifted up by the fountains falls back on the disk within a distance $\Delta R = \pm 0.5$ kpc from the place where the fountain originated. As a consequence, nearly 60% of the metals delivered by the SNe remains within the area where the fountain was formed. This small radial displacement of metals in the disk is in agreement with recent chemical models of the Milky Way (Cescutti et al. 2007).

• We have also found from the simulations that the metal pollution of the clouds is ~ 0.01 in solar units, therefore, negligible compared to the typical ISM abundance of metals. This implies that the clouds that are formed by the fountains in the halo are only very weakly chemically affected by the SNe.

• Once the material of the clouds rains back onto the disk, we may expect that it will provide the formation of new molecular clouds and supersonic filamentary structures that will feed the ISM turbulence, thus closing the gas cycle between the disk and the halo (e.g., de Avillez & Breitschwerdt 2005).

• We have also performed hybrid simulations including both the ejected material from fountains triggered by SNe arising within the galactic disk and the infall of gas accreted from the IGM at a $dM/dt = 1$ to 2 $M_\odot$ yr^{-1} rate (see Figure 7). In this case, the formation of low-metallicity, high-velocity halo structures falling on the disk from the highest latitudes (like the HVCs) is a straightforward consequence.

A final remark is in order. In the study reviewed here, we have included all the essential ingredients of a star-forming disk galaxy, except for the magnetic fields and the thermal conduction effects. The magnetic fields may be significant at helping to lift the fountains and forming, e.g., at least part of the population of HVCs. In fact, large scale magnetic fields with coherent scales of ~ 1 kpc have been observed in the halos of several of these galaxies (e.g., Dettmar 2005). The MHD simulations of galactic fountains by de Avillez & Breidtschwerdt (2005) have produced halo magnetic fields, but with smaller scales. MHD effects have also been invoked by de Gouveia Dal Pino & Medina-Tanco (1999) to accelerate SNe-triggered winds in SB galaxies by a magnetocentrifugal process and more recently, Otmianowska-Mazur, Kowal, & Hanasz (2007) (see also Otmianowska-Mazur et al. 2009) have investigated the joint action of both the Parker-Rayleigh-Taylor instability in a galactic dynamo and the production of cosmic rays by SNe to explain the ascension of large scale magnetic fields to the halo. These effects could also provide guidance and acceleration for the fountains and help the formation of clouds at higher latitudes than those allowed by purely hydrodynamical simulations. Concerning the effects of thermal conduction, these can be highly important at suppressing thermal instabilities and thus structure formation, particularly at the smallest scales (not addressed in the present study). On the other hand, conduction might be inhibited by stochastic magnetic fields. These important ingredients will be considered in future work.

REFERENCES

Bland-Hawthorn, J., & Cohen, M. 2003, ApJ, 582, 246

Bregman J. N. 1980, ApJ, 236, 577

Cappellaro, E., Turatto M., Tsvetkov, D. Y., Bartunov, O. S., Pollas, C., Evans, R., & Hamuy, M. 1997, A&A, 322, 431

Cescutti, G., Matteucci, F., François, P., & Chiappini, C. 2007, A&A, 462, 943

Cooper, J. L., Bicknell, G., Sutherland, R. S., Bland-Hawthorn, J. 2008, ApJ, 674, 157

de Avillez, M. A. 2000, MNRAS, 315, 479

de Avillez, M. A., & Berry, D. L. 2001, MNRAS, 328, 708

de Avillez, M. A., & Breitschwerdt, D. 2005, A&A, 436, 585

de Gouveia Dal Pino, E. M., & Medina-Tanco, G. A. 1999, ApJ, 518, 129

de Gouveia Dal Pino, E. M., Melioli, C., D'Ercole, A., Brighenti, F. & Raga, A. C. 2008, arXiv:0803.3835

Dettmar, R.-J. 2005, in AIP Conf. Proc. 784, Magnetic Fields in the Universe: from Laboratory and Stars to Primordial Structures, ed. E. M. de Gouveia Dal Pino, G. Lugones, & A. Lazarian (Melville: AIP), 354

Dettmar, R.-J., & Soida, M. 2006, Astron. Nachr., 327, 495

Fraternali, F., & Binney, J. J. 2006, MNRAS, 366, 449

González, R. F., de Gouveia Dal Pino, E. M., Raga, A. C., & Velazquez, P. F. 2004, ApJ, 600, L59

Higdon, J. C., & Lingenfelter, R. E. 2005, ApJ, 628, 738

Kahn, F. D. 1981, Investigating the Universe, ed. F. D. Kahn (Dordrecht: Reidel), 1

Konstantopoulos, I. S., Bastian, N., Smith, L. J., Trancho, G., Westmoquette, M. S., & Gallagher, J. S., III 2008, ApJ, 674, 846

Koo, B.-C., & McKee, C. F. 1992, ApJ, 388, 93

Korpi, M. J., Brandenburg, A., Shukurov, A., & Tuominen, I. 1999, A&A, 350, 230

Mac Low, M.-M., McCray, R., & Norman, M. L. 1989, ApJ, 337, 141

Melioli, C., & de Gouveia Dal Pino, E. M. 2004, A&A, 424, 817

Melioli, C., de Gouveia Dal Pino, E. M., & Raga, A. 2005, A&A, 443, 495

Melioli, C., Brighenti, F., D'Ercole, A., & de Gouveia Dal Pino, E. M. 2008a, MNRAS, 388, 573

Melioli, C., Brighenti, F., D'Ercole, A. & de Gouveia Dal Pino, E. M. 2008b, MNRAS, in press (arXiv:0903.0720)

Otmianowska-Mazur, K., Kowal, G., & Hanasz, M. 2007, ApJ, 668, 110

Otmianowska-Mazur, K., et al. 2009, RevMexAA (SC), 36, CD266

Raga, A. C., Navarro-González, R., & Villagrán-Muniz, M. 2000, RevMexAA, 36, 67

Raga, A. C., de Gouveia Dal Pino, E. M., Noriega-Crespo, A., Mininni, P., & Velázquez, P. F. 2002, A&A, 392, 267

Shapiro, P. R., & Field, G. B. 1976, ApJ, 205, 762

Tomisaka, K. 1998, MNRAS, 298, 797

Veilleux, S., Cecil, G., & Bland-Hawthorn J. 2005, ARA&A, 43, 769

Wolfire, M. G., McKee, C. F., Hollenbach, D., & Tielens, A. G. G. M. 2003, ApJ, 587, 278